BIULETYN WAT
ROK XLVIII, NR 6, 1999

Radiation Defects in some Oxide Compounds

SŁAWOMIR MAKSYMILIAN KACZMAREK

Military University of Technology, Instytut Optoelektroniki WAT,
00-908 Warszawa, ul. S. Kaliskiego 2

Abstract. Yttrium-aluminum garnets, yttrium aluminum perovskite, strontium and barium lanthanum and gadolinium gallates, lithium niobate and tantalate as-grown crystals and doped by diffusion with rare-earth (Nd, Dy, Er, Tm, Ho, Pr, Ce, Eu) and ions of the first transition series (Mn, Cr, Cu, Fe) were investigated optically and using Electron Spin Resonance method before and after gamma, electron and proton irradiation.
Keywords: oxide compounds, absorption, additional absorption, luminescence, thermoluminescence, ionizing radiation
Universal Decimal Classification: 548.4

1. Introduction

Among many defects arising during the crystal growth of oxide compounds, a variety of defects are observed: facets, growth striations, dislocations, low angle boundaries, twins, color centers , dislocations with strain field, vacancies, cellular structure, inclusions and cracks [1]. Among these defects, point defects in a given crystal can be sources of new, radiation defects during its application in devices working in external radiation fields. Output characteristics of these devices change (e.g. lasers) in an obvious manner. However, positive effect of radiation defects on output characteristics of some materials is also known [2, 3].

It is difficult to define the nature of color centers. Sometimes these defects are related to impurities although their level may be lower than 10^{-6} weight % while sometimes they are due to oxygen nonstoichiometry or change in cation balance.

The main purpose of our work was to determine the radiation induced defects in $Y_3Al_5O_{12}$ (YAG), $YAlO_3$ (YAP), $SrLaAlO_4$ (SLAO), $SrLaGaO_4$ (SLGO4),

$CaNdAlO_4$ (CNAO), $SrLaGa_3O_7$ (SLGO), $BaLaGa_3O_7$ (BLGO), $SrGdGa_3O_7$ (SGGO), $LiTaO_3$ (LT) and $LiNbO_3$ (LN) single crystals doped with rare-earth and ions of the first transition series.

2. Experimental

The ESR spectra of the single crystals were recorded at 9.4 GHz in the temperature range from 4 K to 300 K using a BRUKER ESP -300 X-band spectrometer.

To study of radiation-induced changes in optical properties of the Nd: YAG crystals, polished in both sides, parallel-plate samples of thickness from 0.5 to 3 mm were prepared. The absorption spectra were taken at 300 K in the spectral range between 4500 and 500 cm^{-1} using a FTIR spectrometer (IFS 113V BRUKER) and in the range 190-1100 nm using a LAMBDA 2 spectrometer (Perkin-Elmer). Fluorescence and excitation spectra were obtained using an ILA-120 3W argon ion laser. The spectra were recorded using a GDM-1000 monochromator with dispersion of 11 cm^{-1}/mm and detected by a RCA C-31034-02 cooled AsGa photomultiplier. For data acquisition the SR 400 photon counting system, controlled with a PC computer, was used.

Radioluminescence spectra were measured in the range 200-850 nm using excitation with X-rays (DRON, 35 kV / 25 mA) and Spectrograph: ARC SpectraPro-500i (Hol-UV 1200 gr/mm grating and 500 nm blazed grating 1200 gr/mm, 0.5 mm slits), PMT: Hamamatsu R928 (1000 V).

The samples prepared for the thermoluminescence (TL) studies, with the thickness lower that 1 mm and with the diameters up to 6 mm, were not polished. Measurements of the TL of „as grown" crystals as well as those for γ-irradiated ones were performed in the temperature range from 70 to 400^oC by means of a roundabout-type WAWA-TLD RA'95 analyzer.

Three different sources of radiation were used: (1) γ-irradiation at 300 K and 77K, (2) electrons with fluencies 10^{14} - 5 x 10^{16} electrons/cm^2 at 77 K, and (3) protons with fluencies 10^{13} - 10^{16} protons/cm^2.

The gamma ray irradiation of the samples was performed with a ^{60}Co source at a rate of 1.5 Gy/s up to an absorbed dose of 10^5 Gy.

Electron irradiations at an energy of 1 MeV were performed using a Van de Graaf accelerator.

Proton exposures were done with the use of a C30 cyclotron at an energy of 21 MeV. Each time the fluency was measured with a charge integrator. To avoid the sample overheating the average beam current was kept at approximately 200 nA. The irradiated samples were investigated in the gamma energy range 40 keV - 4 MeV using a precise Hewlett Packard Ge(Li) gamma spectrometer of high efficiency (Ge(Li) crystal volume: 77 ccm). As a rule, gamma measurements

were performed next day after the irradiation, which was necessary to avoid the overloading the detector by short-lived activity of the samples. Thus, only gamma lines belonging to rather long-lived isotopes were recorded.

Values of ΔK(λ) factors which describe an additional absorption due to the irradiation were calculated according to the formula:

$$\Delta K(\lambda) = \frac{1}{d} \cdot \ln \frac{T_1}{T_2}, \tag{1}$$

where K is absorption, $\Delta K(\lambda)$ is the additional absorption, λ is the wavelength, d is the sample thickness, and T_1 and T_2 are the transmissions of the sample measured before and after irradiation, respectively.

3. Color centers in $ABCO_4$ crystals

Lanthanum gallate and lanthanum aluminate seem to be suitable substrates for thin film epitaxial growth of the high temperature superconductors $YBa_2Cu_3O_{7-d}$ and $La_{2-x}Sr_xCuO_4$ [1]. The interest in these materials stems from their crystal structure, lattice constant and dielectric properties. Thus changes in their structure under influence of external field, e.g. thermal and radiation, are very important observations for a later application.

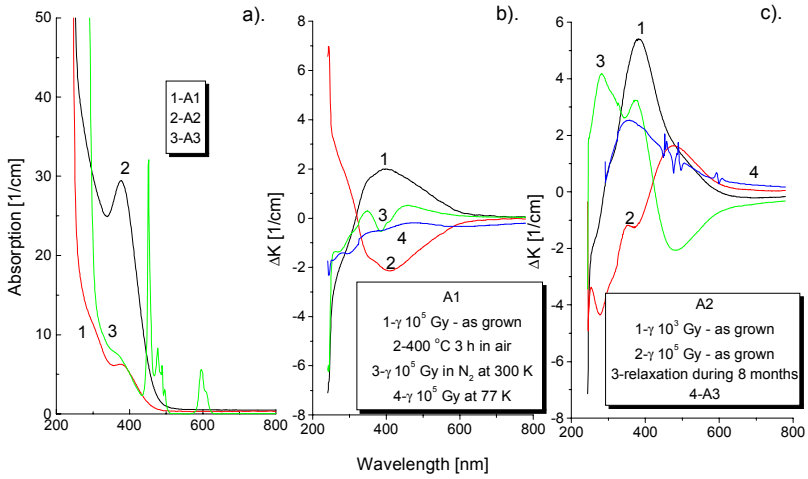

Fig. 1. (a) absorption and (b, c) additional absorption in pure (A1 and A2 samples) and Pr^{3+} (6 at.%) doped (A3 sample) $SrLaAlO_4$ single crystals after γ-irradiation with doses 10^3-10^5 Gy. Irradiation was performed for crystals as grown in the following conditions: in air at 300 K (curve 1, Fig. 1b and curves 1,2 and 4 in Fig. 1c), in N_2 gas at 300 K (curve 3, Fig. 1b) and in N_2 liquid at 77 K (curve 4, Fig. 1b)

Both SLGO4 and SLAO crystallize in a tetragonal structure similar to that of K_2NiF_4. Crystal lattices contain linked oxygen octahedrally with Al or Ga ions in their center and with Sr and La ions located between them. Therefore, each Al or Ga ion has six oxygen ions in their first coordination zone and nine Sr or La ions in their second coordination zone. Additionally, it is usually assumed that Sr and La are randomly distributed between oxygen octahedra.

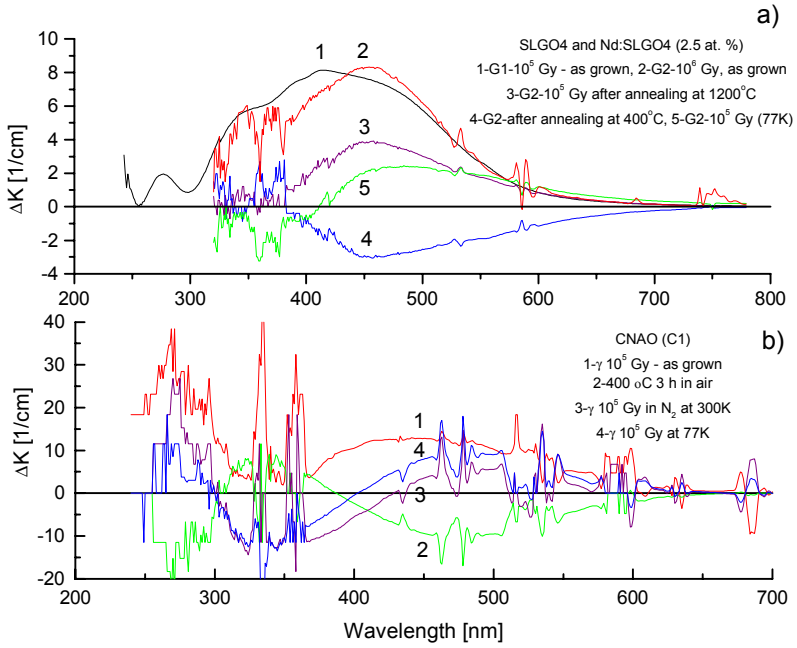

Fig. 2. Additional absorption in (a) pure (G1 sample) and Nd^{3+} (2.5 at.%) doped (G2) $SrLaGaO_4$ and (b) $CaNdAlO_4$ (C1 sample) single crystals after γ-irradiation with a dose of 10^5 Gy.

Fig. 1 presents additional absorption bands in two undoped SLAO samples (A1 and A2 samples) coming from two different crystal growth runs and an SLAO sample doped with Pr^{3+} - 6 at.% - A3 sample. The γ-irradiation were performed on as grown crystals: in air at 300 K (curve 1, Fig. 1b and curves 1,2 and 4 in Fig. 1c), in N_2 gas at 300 K (curve 3, Fig. 1b) and in N_2 liquid at 77 K (curve 4, Fig. 1b). As seen from curves 1 and 2 in the Fig. 1a, undoped SLAO exhibit different value of absorption spectrum with maximum at 381 nm, equal to 5.5 and 30 cm^{-1} for samples 1 and 2, respectively, although additional absorption after γ-irradiation with a dose of 10^5 Gy is the same (2 cm^{-1}) - see curve 1 in Fig. 1b and curve 2 in Fig. 1c. Moreover, the shape of the additional absorption changes with an increase in dose and the position of the maximum shifts towards a longer

wavelength of 476 nm (see curve 3 in Fig. 1b and curve 2 with respect to curve 1 in Fig. 1c). The position and the value of the maximum also depend on the type of impurity (358 nm and 2.5 cm^{-1} for A3 sample, curve 4 in Fig. 1c). It was found that annealing at room temperature for 8 months returned the optical characteristics to the initial type (curve 3 in Fig 1c). Similarly, annealing at 400^{o}C for 3 h in air leads to the same effect (see curve 1 and curve 2 in Fig. 1b). Irradiation with gamma's performed at 77 K does not introduce new defects compared to 300 K (compare curve 4 and curve 3 in Fig. 1b).

Two samples of SLGO4 crystal (Fig. 2) were investigated after the following treatments: G1 as grown sample (pure SLGO4) was irradiated with γ 10^5 Gy at 300K in air (curve1). G2 as grown sample (Nd^{3+} doped - 2.5 at.% - SLGO4) was irradiated with γ 10^6 Gy in air (curve 2), annealed at 1200 ^{o}C and irradiated with γ 10^5 Gy in air (curve 3), next annealed in air for 3 h at 400 ^{o}C (curve 4) and irradiated with γ 10^5 Gy at 77 K (curve 5).

Pure SLGO4 crystal has the maximum value of additional absorption after γ 10^5 Gy at 415 nm (about 8 cm^{-1}, curve 1) but neodymium doped at 453 nm (about 8 cm^{-1}, curve 2). After annealing the crystal at 1200^{o}C for 3 h the value of the maximum decreases (curve 3). Further annealing at 400^{o}C of the γ-irradiated sample fully reconstructs absorption spectrum (curve 4). Irradiation of the crystal in liquid nitrogen temperature with the same value of the dose shifts the maximum towards longer wavelengths and decreases its value (curve 5).

The ESR lines which we observed in SLAO and SLGO4 crystals, called as „D"-defects [4], depend on the crystal coloration. Most intensive ESR lines were observed for dark-green single crystals and decreased for green and yellow crystals. For colorless crystals no ESR lines were measured.

After γ-irradiation of CNAO crystals (Fig. 2b) one wide additional absorption band is observed (see curve 1) with a maximum at 420 nm (12.5 cm^{-1}), which changes in intensity and position after subsequent thermal and radiation treatments. Annealing at 400^{o}C shifts the maximum towards a longer wavelength of 470 nm (curve 2). Subsequent γ-irradiation performed at 300 K and 77 K does not change position of the maximum (see curve3 and curve 4), but gives smaller values of additional absorption in comparison with the first irradiation (curve 1).

4. LN and LT single crystals

Lithium niobate crystals doped by rare-earth and transition ions have attracted attention as self-frequency doubling and Q-switched lasers because of the possibility for combining the laser emission and non-linear properties of the matrix in a single medium.

As seen from Fig. 3a most effective diffusion is observed in the case of LT crystal and for a temperature of 900^{o}C. Diffusion process lead to a large increase in

the optical density of the crystal in the UV range of a spectrum (Fig. 3b). Concentration of the impurity incorporated during diffusion increases with the duration of diffusion and an increase in a temperature (see Fig. 3a).

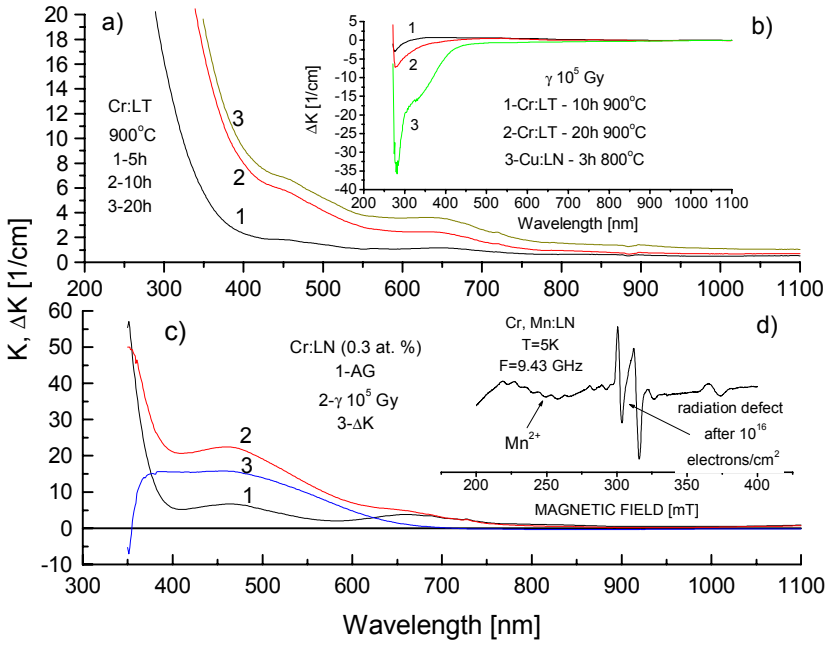

Fig. 3. Absorption (a) for LT, additional absorption (b) for LT and LN crystals doped by diffusion with Cr and Cu, after γ irradiation with a dose of 10^5 Gy, absorption and additional absorption (c) in LN crystals doped during growth with Cr after γ-irradiation with a dose of 10^5 Gy and, ESR spectrum (d) of Cr doped LN single crystal irradiated with electrons with a fluency of $5*10^{16}$ cm^{-2}

Doping during crystal growth with chromium introduces many point defects in the LN crystal [5] and is revealed after γ-irradiation as at least two additional absorption bands at 381 nm and 464 nm; 15 cm^{-1} (Fig. 3c, curve 3). The second band suggests a recharging effect of chromium ions in the LN lattice. After electron or γ-irradiation of LN crystals doped with Cr, a new ESR spectrum having 3 anisotropy lines with Lande coefficient, g, equal to 2 is observed (see Fig. 3d). Moreover, irradiation of the crystals with electrons leads to a decrease in the intensity of Mn^{2+} lines (noncontrolled impurity) while γ-irradiation do not change this intensity [6].

In Fig. 4 absorption and additional absorption in (a) LT, Nd: LT (0.3 at. %), (b) Cu: LN (0.03 and 0.06 at. %), (c) Cr: LN (0.3 at. %) and (d) Fe: LN (0.3 at. %) crystals are presented. In the additional absorption spectrum of LT and Nd: LT single crystals (curves 1 and 2, respectively), two bands are seen: first with

a minimum at 320 nm and second one with a maximum at 400 nm. The first defect leads to the brightness of LT crystals in the range 270-350 nm, connected with some optically active dopant seen in the spectrum of as grown crystal for about 320 nm (may be Fe). Second one, in our opinion, may be connected with F like center.

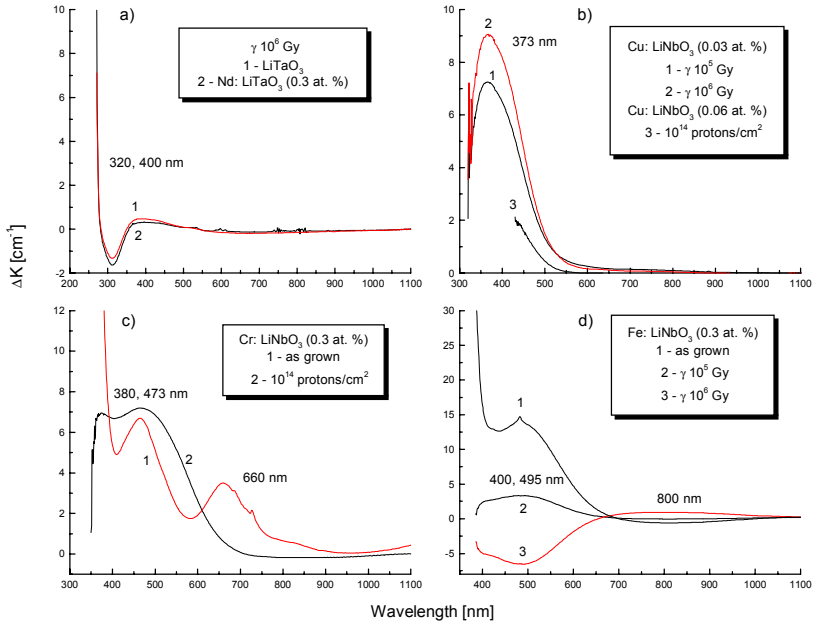

Fig. 4. Absorption and additional absorption in (a) $LiTaO_3$ and Nd: LT, (b) Cu: LN, (c) Cr: LN and (d) Fe: LN single crystals. Additional absorption was registered for gamma quanta with doses 10^5 and 10^6 gy and for protons with a fluency of 10^{14} cm^{-2}

For all LN crystals a change of the fundamental absorption edge is seen with type of doping (Figs 4b, c, d). For Cu: LN crystal only one additional band is observed with a maximum of 373 nm, which is connected probably with F like center (Fig. 4b). An increase in dose leads to an increase in intensity of additional absorption (curves 1, 2). This increase is lower for greater concentrations of copper (curve 3).

In the case of Cr doping one can see two additional absorption bands: at 380 and 473 nm (curve 2, Fig. 4c). The first is connected probably with F like centers and the second with an increase in Fe concentration. Probably, in the phase of the crystal's growing there exists Cr^{2+} ions, which change to Cr^{3+} under ionizing treatment (curve 1).

Similar situation takes place for Fe: LN crystal (curve 2, Fig. 4d). After gamma irradiation with a dose of 10^5 Gy two bands arises with maxima at: 400 and 495 nm. The first is connected with F like centers and the second with an increase in Fe^{3+} ions concentration (curves 1 and 2). In Fig. 4d appreciable discrepancy is seen for Fe doped LN crystal in comparison with previously described LN crystals. After gamma irradiation with a dose of 10^6 Gy the radiation annealing is seen (curve 3, Fig. 4d) and the arising of a new band with a maximum at about 800 nm. This band is connected with absorption band existing in absorption spectrum of as grown crystal (curve 1, Fig. 4d).

5. SLGO and BLGO crystals

ABC_3O_7 melilite crystals are characterized by relatively high structural homogeneity and good lasing properties. Undoped single crystals are successfully used as substrates for high temperature superconducting layers, while doped with Nd, Pr and Dy as laser materials.

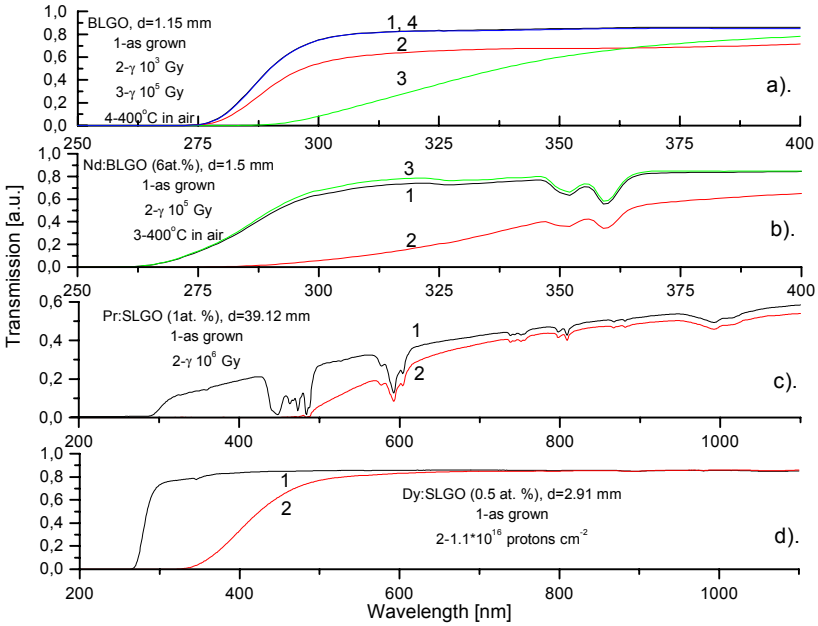

Fig. 5. Change in transmission of (a) undoped BLGO, (b) Nd: BLGO, (c) Pr: SLGO (c) and (d) Dy: SLGO single crystals after γ-rays (a-c) and protons (d)

In BLGO and SLGO single crystals undoped and doped with rare-earths, both for gamma, electron and proton irradiation an intense (30 cm^{-1}) additional absorption band near 270 nm and, related with it, a new anisotropy ESR spectrum, marked as "G" type defect, was observed. Moreover, 370 nm band associated probably with oxide vacancies [7]. Angular dependencies measured for different planes suggested that the observed lines are connected with oxide tetrahedral: four non-equivalent paramagnetic centers are seen.

a)

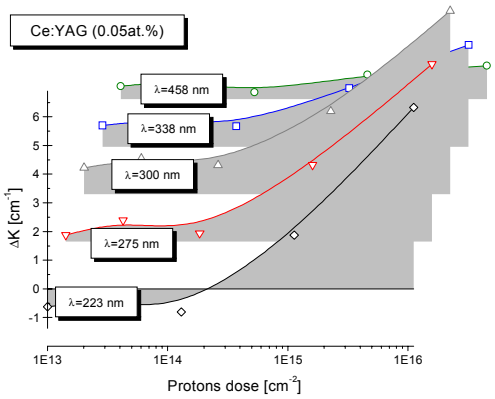

b)

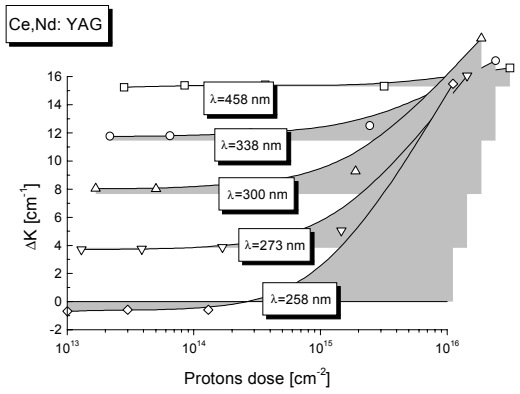

Fig. 6. Dose dependencies of protons irradiated YAG: Ce (a) and YAG: Ce, Nd single crystals for several values of wavelengths and fluencies between 10^{12} and 10^{16} cm^{-2}

At room temperature these lines disappear after about 1 month from γ-irradiation. It was assumed that paramagnetic centers arises due to electron knock out from O^{2-} ion and further capture it by Ga^{3+} ion [7, 8]. This radiation defect leads to a shift in the short-wave absorption edge towards long wavelengths even by hundreds of nm (Fig. 5). The wavelength for which the transmission value reach the level of 0.001 was taken as a short-wave absorption edge. As seen in the Fig. 5, for BLGO and SLGO crystals, the shift depends on the type of impurity (Fig. 5a, b), value of a dose (Fig. 5a curve 2 and curve 3) and, arises independent on type of the radiation (Fig. 5c - γ and Fig. 5d - protons, curves 2). Annealing of the crystals at 400°C for 3 h in air returned optical characteristics to type before irradiation (Fig. 5a, curve 4 and Fig. 5b, curve 3). The G-type radiation defect was observed for BLGO and SLGO crystals undoped and doped with rare earths and transition ions, but for $SrGdGa_3O_7$ crystals it was observed only in absorption spectrum for doses greater then 10^6 Gy [9].

6. YAG single crystals

YAG crystals are very often applied in optoelectronic devices as lasers and scintillating materials due to their good thermal and mechanical properties.

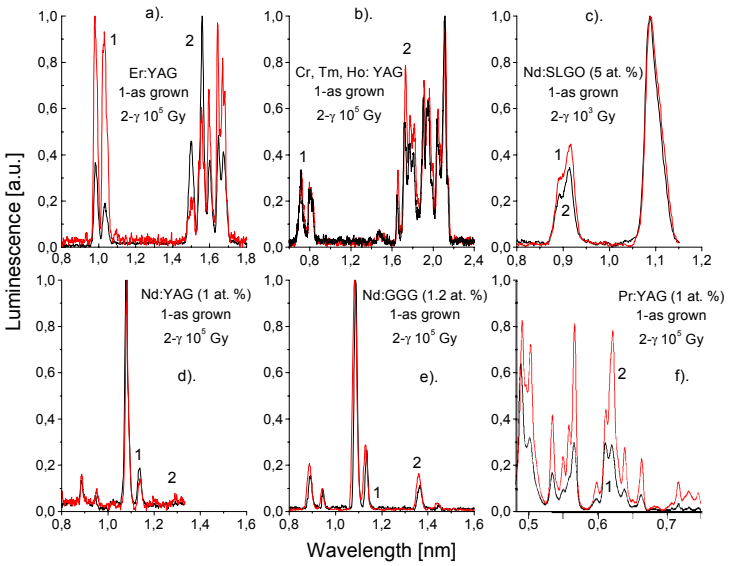

Fig. 7. Changes in the luminescence of (a) Er: YAG, (b) Cr, Tm, Ho: YAG, (c) Nd: SLGO, (d) Nd: YAG, (e) Nd: $Gd_3Ga_5O_{12}$ and (f) Pr: YAG single crystals after γ-rays

After γ-irradiation, pure and rare-earth doped YAG crystals show a wide, complex additional absorption band in the range between 200 and 900nm.

Doping, for example, by neodymium weakly influences the shape of the additional absorption band but cerium behaves inversely. Near 338 and 458 nm (electron transitions in cerium ions) the additional absorption bands arises that suggests recharging effect of cerium ions [10]. Irradiation of the crystals in liquid nitrogen leads to growth of additional absorption bands even three times.

Fig. 6 presents additional absorption, ΔK, as a dose function in YAG: Ce (Fig. 5a) and YAG: Ce, Nd (Fig. 5b) single crystals after irradiation with protons with fluencies from 10^{12} to 10^{16} particles cm^{-2}. In the Fig. 6 there can be distinguished two dose ranges: (1) fluencies less than $5*10^{14}$ cm^{-2} where recharging effects dominate and, (2) fluencies greater than $5*10^{14}$ cm^{-2} where the presence of Frenkel defects is clearly seen.

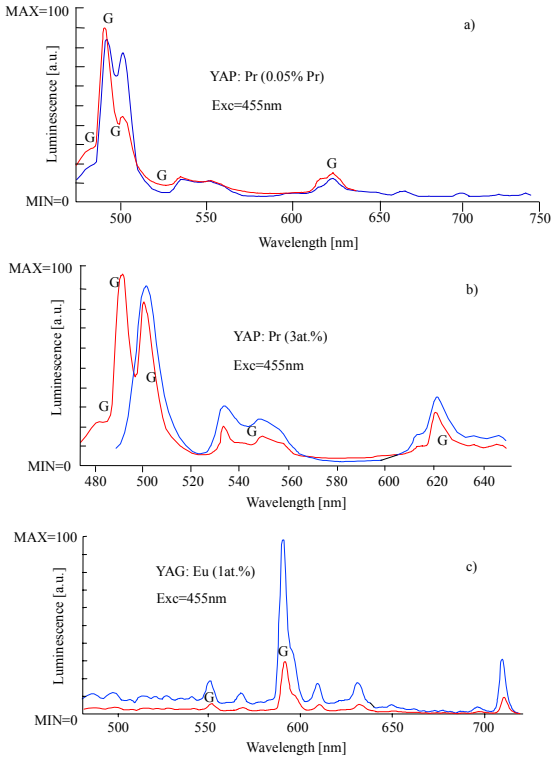

Fig. 8. Changes in the luminescence of (a) YAP: Pr (0.05 at. %), (b) YAP: Pr (3 at. %) and (c) YAG: Eu (1 at. %) after γ-rays with a dose of 10^5 Gy (curves marked by "G")

Figs 7 and 8 present changes in luminescence of YAG crystals doped with Er (Fig. 7a), Cr, Tm, Ho (Fig. 7b), Nd (Fig. 7d), Pr (Fig. 7f) and Eu (Fig. 8c) after γ-irradiation with a dose of 10^5 Gy. One can see large changes in YAG: Er (Fig. 7a) and YAG: Pr (Fig. 7f) crystals. In these figures changes in the luminescence spectrum after γ-irradiation of Nd doped SLGO and $Gd_3Ga_5O_{12}$ crystals (Fig. 7c, e, respectively) and Pr doped $YAlO_3$ (YAP: Pr (0.05 at. %) and YAP: Pr (3 at. %)) crystals are also presented for comparison (Fig. 8a, b, respectively).

These changes are associated with the presence of color centers (e.g. in Er: YAG - see [11-13]) which transfer energy of excitation to e.g. Er ions or valency change of active or sensitizing dopant (for example Ce or Cr in YAG: Ce or Cr, Tm, Ho: YAG crystals, respectively). The above mentioned changes in luminescence spectra have appropriate consequence in emission of the lasers [14].

7. Radioluminescence measurements

Some of the measured oxide compounds does not show any emission during their exciting by X-rays with use of the radioluminescence method. There are high doped with rare-earth's (e.g. 10at. % Nd) $SrLaGa_3O_7$ and $BaLaGa_3O_7$, high doped with Er (33at.%)YAG' s, Cu doped LN and LT single crystals. Among the investigated crystals there are such, in which strong interaction of active ions leads to the decaying of their self-emission, as in the case of Nd (1at.%) doped YVO_4.

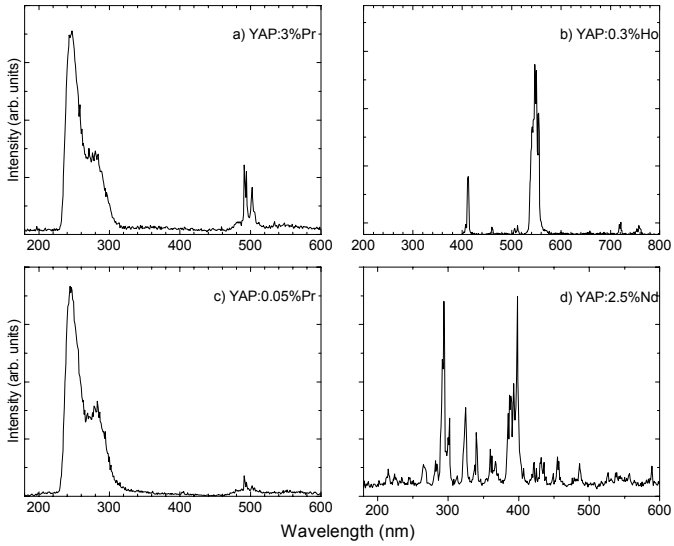

Fig. 9. Radioluminescence spectra of (a) Pr: YAP (3at.%), (b) Ho: YAP (0.3at.%), (c) Pr: YAP (0.05at.%) and (d) Nd: YAP (2.5at.%)

The following impurities are very good seen in the radioluminescence spectrum of the investigated crystals (good energy transfer from lattice ions to dopants): rare-earth's - Pr, Nd, Er, Dy, Tm, Ho, Ce, and transition metals: Cr, Fe. Fig. 9 shows RL intensity for YAP crystals doped with Pr, Ho and Nd.

8. Measurements of γ-spectra

There arises many defects in oxide compounds under proton irradiation. Re-charging effects of non-controlled and active dopants due to e.g. delta electron capture or ionization process, Frenkel defects, clusters and amorphous areas and other [7, 15]. Type of the effects depends on energy and a dose of proton irradiation and susceptibility of a given crystal to protons [7]. The last feature depends on the type and density of active dopant inside oxide crystal and its purity: growth defects, non-controlled impurities and codopants.

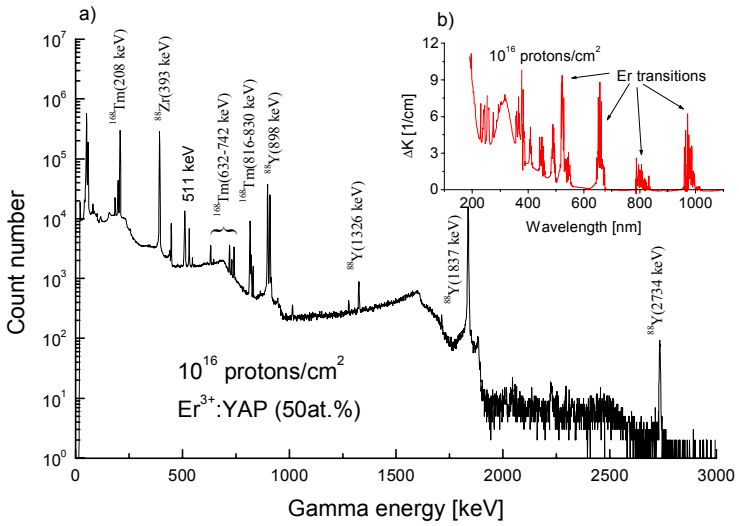

Fig. 10. Gamma spectrum (a) and, additional absorption bands (b) of Er^{3+}:YAP crystal irradiated by protons with a fluency of 10^{16} per cm^2

The aim of these measurements was to look for utility of gamma rays emitted by the nuclear reaction products, both from nuclei in the basic crystal lattice and from dopants, as a possible source of an additional useful information about the crystal itself and produced defects.

In this work we present, as an example, the gamma energy spectra from Er^{3+}:YAP, Cr^{3+}:LN and Cr^{3+}:SGGO samples. Cu^{2+}:LN gamma spectra are of the

same type as for Cr^{3+}:LN, exclude characteristic for the last 1436 keV peak coming from ${}^{52}_{25}Mn$, arising in the reaction ${}^{52}_{24}Cr(p,n){}^{52}_{25}Mn$. In YAG crystals the next nuclear reactions were mainly observed: ${}^{89}_{39}Y(p,pn){}^{88}_{39}Y$ and ${}^{89}_{39}Y(p,2n){}^{88}_{40}Zr$. In Cr: SGGO crystal the next nuclear reactions were stated: ${}^{155}Gd(p, n){}^{155}Tb$, ${}^{156}Gd(p, n){}^{156}Tb$, ${}^{160}Gd(p, n){}^{160}Tb$, ${}^{88}Sr(p, n){}^{88}Y$, ${}^{69}Ga(p,2n){}^{68}Ge$.

In Fig. 10a gamma spectrum of Er^{3+}:YAP crystal irradiated by protons with a fluency of 10^{16} per cm^2 is shown. All peaks in the spectrum arise from the decay of isotopes produced in reactions Y(p, pn)Y, Y(p,2n)Zr, and Er(p, n)Tm. Gamma lines from reactions on Yttrium nuclei belonging to the ideal crystal lattice are clearly visible as well as those from reaction on dopant Erbium nuclei. In the presented sample the content of the Er atoms was relatively high (50 at. %).

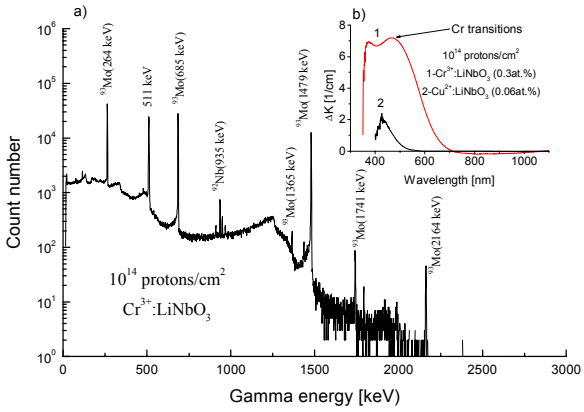

Fig. 11. gamma spectrum (a) of Cr^{3+}:LN (0.3at.%) crystal and, additional absorption (b) of Cr: LN (0.3 at. %) and Cu: LN (0.06 at. %) crystals after proton irradiation with the fluency of 10^{14} per cm^2

In Fig. 10b AA spectrum after proton irradiation with the fluency of 10^{14} cm^{-2} can be seen. Beside typical additional absorption bands additional transitions inside Er^{3+} ions can be observed.

Fig. 11a shows gamma spectrum of Cr: LN after proton irradiation with the fluency of 10^{14} per cm^2. The peaks in the spectrum arise from the decays of isotope of ^{93}Mo produced in the reaction ^{93}Nb(p, n) and ^{92}Nb from ^{93}Nb(p, pn)^{92}Nb. In this spectrum we do not observe clearly visible peak belonging to the isotope from the reaction with dopant nuclei Cr.

Fig. 11b presents additional absorption for Cr: LN (curve 1) and Cu: LN (curve 2) crystals after proton irradiation with a fluency of 10^{14} cm^{-2}.

Fig. 12 shows (a) gamma spectra and (b) additional absorption band registered for Cr: SGGO crystal after proton irradiation with a fluency of 10^{14} cm^{-2}. In the absorption spectrum only Cr^{4+} ion transitions are seen [9]. After proton irradiation

concentration of Cr^{4+} ions decreases (negative values of AA in the range of 650-900 nm) as an effect of $Cr^{4+} \rightarrow Cr^{3+}$ reaction, and two new bands arises: at about 300 nm and at about 600 nm. First is associated with G type paramagnetic defect ($Ga^{3+} \rightarrow Ga^{2+}$) [9], whereas second one with electron transitions inside Cr^{3+} ions. So, under proton irradiation there arises new defect (G) and changes in concentration of Cr^{3+} ions are observed.

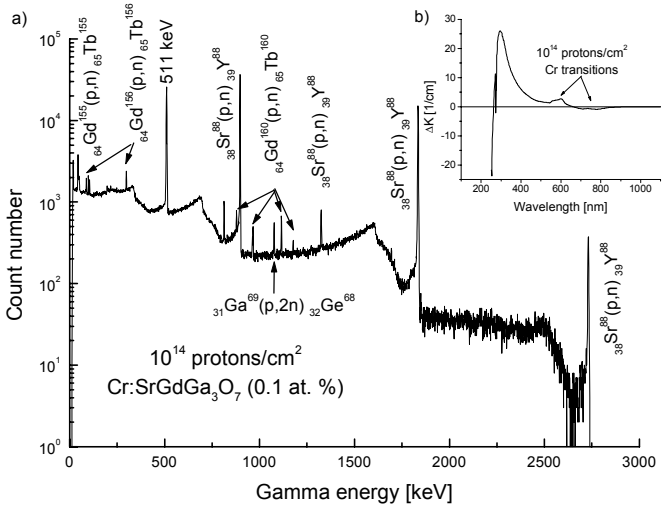

Fig. 12. Gamma spectra (a) and, additional absorption (b) of Cr: SGGO single crystal after proton irradiation with a fluency of 10^{14} cm^{-2}

Spectroscopic investigations has shown that under proton irradiation recharging processes take place in YAG, YAP, SGGO and LN crystals for doses up to 10^{14} cm^{-2}. There are associated with point defects arising in „as grown" crystals and undergo to saturation phenomenon. Changes in valency of the next active ions were observed: Er in YAP: Er^{3+} crystals, Ce in YAG: Ce^{3+} or YAG: Ce^{3+},Mg^{2+} crystals, Cr in LN: Cr^{3+} and SGGO: Cr^{4+} crystals. Moreover, F-centers and paramagnetic defects formation was stated for LN, YAG and SGGO crystals.

The accuracy of the intensity measurement of 0.208 MeV gamma line from ^{167}Tm for the Er^{3+}:YAP crystal is 0.14%, including the statistical and systematic errors. Extrapolating above result to the lower limit of Er content, one can expect the level of about 0.1at.% is still safely detectable Er level in the crystal.

It seems that in the future gamma lines can serve two purposes:

(i) To estimate the relative contributions of two different nuclear processes: elastic proton scattering and nuclear reactions, both leading to some Frenkel defects, which can correlate with observations of particular optical effects in the same sample,

(ii) To measure, after preliminary absolute calibration, the level of the e.g. Er dopant in the crystal. The correct numerical procedure allowing to get the absolute value of the admixture contamination should include proper averaging over the proton energy varying along its trajectory in the sample. Here, we only estimate the statistical accuracy of measurement of particular gamma line intensities having in mind only relative measurements.

Generally, to determine the lower level of dopant detectable under proton irradiation, some additional measurements involving life-time of the reaction product and intensity ratios of gamma spectrum are necessary.

Concerning the nuclear reaction induced defects, their presence can be experimentally recognized because they often contain the radioactive final nuclei, which can be detected by measurements of gamma rays (see Figs 10 - 12). An appearance of the particular gamma lines characteristic for some radioisotope is detected using one of standard gamma-spectrometric methods. On the other hand, the quantitative interpretation of such spectra, having in mind the production of particular optically active defects in the lattice is rather complex and is in its beginning stage.

9. Thermoluminescence and ESR measurements

Fig. 13 shows thermoluminescence measurements for BLGO and BLGO: Nd (curves 1 and 2 in Fig. 13a -after 10^3 Gy and curves 1 and 2 in Fig. 13b - 1.5 month after 10^5 Gy, respectively), SLGO (Fig. 13c - as grown crystal, curve 1, after 10^3 Gy, curve 2 and 1.5 month after 10^5 Gy, curve 3), YAG: Nd (Fig. 13d - after γ 10^3 Gy and Fig. 13e - for as grown crystal) and, LN: Dy (Fig. 12f - after 10^3 Gy, curve 1 and 1.5 month after 10^5 Gy, curve 2) single crystals. Radiation defects created in these crystals by gamma rays may be seen and their change with time (relaxation process). More strong radiation defect (measured as a maximum of thermoluminescence intensity) show BLGO and YAG crystals. YAG crystals exhibit at least two radiation defects while SLGO and BLGO crystals only one.

In the case of YAG: Nd crystals, at the heating rate of 3 K/s there are three peaks at about 462, 517 and 563 K. In the frame of a simple model of Randall and Wilkins, the peaks are associated with the three different electron traps. To find the trap parameters we used the Randall-Wilkins formula [17]:

$$I(T) = \sum_{i=1}^{4} n_{0i} s_i \exp\left(-\frac{E_i}{k_B T}\right) \exp\left(-\frac{s_i}{\beta} \int_{T_o}^{T} \exp\left(-\frac{E_i}{k_B T}\right) dT\right) \qquad (2)$$

where $I(T)$ is the thermoluminescence intensity at the temperature T, β is the heating rate, n_0 the initial concentration of filled traps, E the trap depth, s the frequency factor, and k_B is the Boltzmann constant. This expression was fitted to

the experimental points for YAG: Nd. A detailed description of the fitting procedure is given by [18]. The results of the fit are summarized in Table 1. The thermoluminescence of LN: Dy (Fig. 13f) crystal exhibit many narrow peaks. Comparing Figs 13a,b and 13c it may be seen the greater stability of radiation defects in SLGO than in BLGO crystals.

Table 1

The depths and frequency factors of the traps in YAG: Nd crystal.

trap	E [eV]	ln s
1	1.0	23.5
2	1.1	23.1
3	2.6	51.1

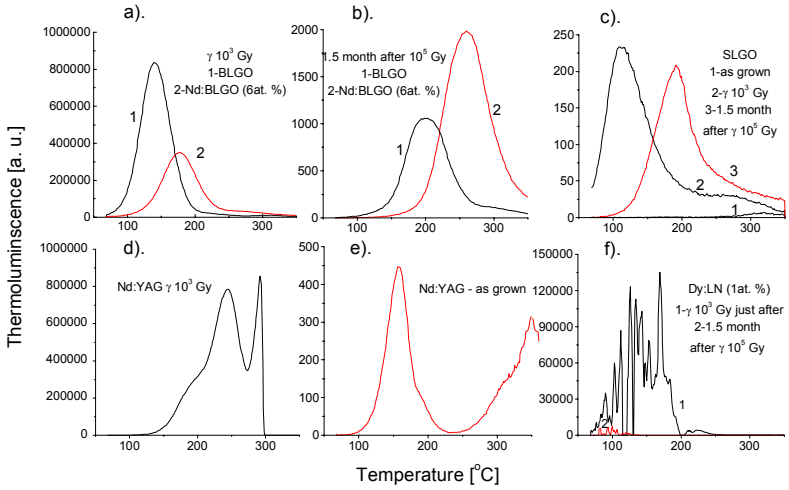

Fig. 13. Thermoluminescence of (a, b) BLGO and BLGO: Nd, (c) SLGO, (d, e) YAG: Nd, (f) LN: Dy single crystals after γ-irradiation with doses 10^3-10^5 Gy

Fig. 14 illustrates the same radiation defects created in SLGO (Fig. 14a), BLGO (Fig. 14b) and LN: Cr, Mn (Fig. 14c) crystals observed by means of ESR technique. As seen from the figure radiation defect is revealed by new ESR lines (for example G1 line, for SLGO, Fig. 14a), which relax with time (Fig. 14b for BLGO crystals) and whose intensity depends on the irradiation dose while the shape on the temperature (Fig. 14b). Presented in Fig. 14 defects arises for all types of applied radiation, gamma's (Fig. 14 a,b) and electrons (Fig. 14c).

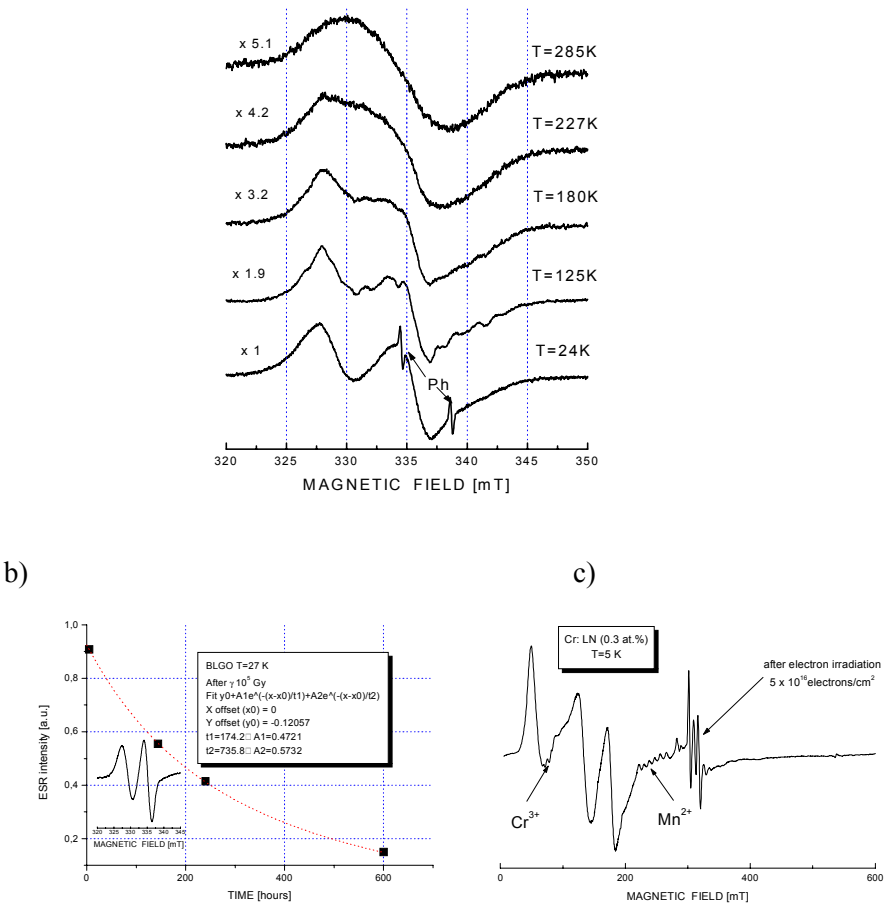

Fig. 14. ESR results in (a) SLGO, (b) BLGO and (c) LN: Cr single crystals after irradiation with gamma's or electrons

10. Summary

10.1 $ABCO_4$ single crystals

In the case of $ABCO_4$ crystals it has been found that the main reason for defects formation is oxygen vacancy. Some growth planes of crystals have similar value of the attachment energy and some of them contain a great number of oxygen ions with weak bonding. Therefore, small changes in growth conditions affect the

oxygen defects. After γ irradiation, in $ABCO_4$ single crystals additional absorption bands arise with their maxima at a level of 10 cm^{-1}, showing a tendency to change their shape and intensity with a change of the dose. This means that investigated crystals are radiationally unstable.

10.2 LN and LT crystals

With the growth of impurity concentration the fundamental optical absorption edge remains unchanged (270 nm) for LT but changes for LN crystals doping by diffusion. Cr doping of these crystals by diffusion leads to an increase in the absorption density in the UV-range, while doping during crystal growth leads to an increase in the absorption density mainly in the VIS-range. Irradiation of the crystals with gammas leads to clearing of their absorption spectrum (-35 cm^{-1} for Cu: LN crystal), especially in the UV region, for LN crystals doped by diffusion and, to coloring (15 cm^{-1}), especially in the VIS region, for LN crystals doped during growth. This means that Cr doped by diffusion LN crystals exhibit lower level of defect content than doped during growth.

Doping during growth with chromium introduces many point defects and is revealed after γ-irradiation as at least two additional absorption bands at 380 nm and 473 nm. The second band suggests a recharging effect of chromium ions in the LN lattice. It is possible that Cr^{2+} ions are present in as grown crystals. This supposition is confirmed by a value of additional absorption (about 15 cm^{-1}) which suggests high level of defect content in the LN crystal. Similar situation takes place for Fe: LN crystals.

After electron or γ-irradiation of LN crystals doped with Cr, a new ESR spectrum having 3 anisotropy lines is observed. Obtained angular dependencies are ambiguous due to the overlapping of Cr and paramagnetic peak lines. For this reason determination of peak localization was not possible.

10.3 SLGO, BLGO and SGGO single crystals

In SLGO, SGGO or BLGO crystals doped with Pr, Dy and Nd as well as undoped ones, after γ or proton irradiation, the additional absorption bands appear in the absorption spectra with the maxima at about 270 and 370 nm. For SLGO and BLGO crystals the first band shifts the short-wave absorption edge of the crystal towards the longer wavelengths. This shifting depends on the type of impurity, irradiation dose and has similar character for gammas and protons for doses up to 10^6 Gy and fluency up to 10^{14} protons/cm^2, respectively. We have shown that this optical effect is connected with paramagnetic “G” center placed in oxide tetrahedral around Ga^{3+} ion. It was assumed that paramagnetic centers arises due to electron knock out from O^{2-} ion and further capture it by Ga^{3+} ion, which changes into paramagnetic Ga^{2+}.

10.4 YAG and YAP single crystals

After γ-irradiation, pure and rare-earth doped YAG crystals show a wide, complex additional absorption band (color centers) in the range between 200 and 900nm. The obtained results point to the direct influence of the color centers on the processes of formation of the inverse population of the energy levels of Er: YAG (positive), Cr, Tm, Ho: YAG (positive) and Nd: YAG (negative) lasers. Gamma irradiation leads to the formation of color centers which transfer energy of excitation to excited laser level (as in the case of Er: YAG or Er: YAP laser) and also to an increase in active impurity concentration and thus luminescence intensity, e.g. for Ce: YAG and Cr, Tm, Ho: YAG (Cr) crystals.

From additional absorption after proton irradiation performed for Ce: YAG and Ce, Nd: YAG crystals results that there can be distinguished two dose ranges: (1) fluencies less than $5*10^{14}$ cm^{-2} where recharging effects dominate and, (2) fluencies greater than $5*10^{14}$ cm^{-2} where the presence of Frenkel defects is clearly seen. The same result we have obtained for SLGO crystals doped with Dy.

Accuracy of the intensity measurement of 0.208 MeV gamma line from ^{167}Tm in Er^{3+}:YAP crystal, arising after ionizing this crystal by protons, permit to measure of Er content in YAP single crystal. We expect that the level of about 0.1at.% is still safely detectable Er level in the crystal. Possible energy transfer from color centers to Er ion in this crystal is described in [12].

ACKNOWLEDGMENTS

I wish to acknowledge the assistance of I. Pracka, T. Łukasiewicz, J. Kisielewski, Z. Frukacz from the Institute of Electronic Materials Technology (Warsaw) and M. Berkowski from the Institute of Physics Polish Academy of Sciences (Warsaw) with preparation of crystals used to investigations, Z. Moroz and J. Wojtkowska from the Institute of Nuclear Studies in Świerk with proton irradiations, S. Warchoł from the Institute of Nuclear Chemistry and Technology (Warsaw) with electron and γ-irradiations, R. Jabłoński from the Institute of Electronic Materials Technology with ESR investigations, R. Piramidowicz from the Institute of Microelectronics and Optoelectronics Technical University (Warsaw) and M. Kwaśny from the Institute of Optoelectronics Military University of Technology (Warsaw) with luminescence measurements and W. Drozdowski from the Institute of Physics Nicolae Copernicus University (Toruń) with radioluminescence and thermoluminescence measurements.

Received August 25, 1998; revised February 25, 1999

REFERENCES.

[1] A. Pajączkowska, Proc. of SPIE, 2373 (1995) 2.

[2] M.R. Bedilov, H.B. Beisembaieva, M.S. Sabitov, Kwantowa Elektronika, 21 (1994) 1145.

[3] S.M. Kaczmarek, A.O. Matkovskii, Z. Mierczyk, K. Kopczyński, D.J. Sugak, Optoelectronics Review, 3/4 (1995) 74.

[4] A. Gloubokov, R. Jabłoński, W. Ryba-Romanowski, J. Sass, A. Pajączkowska, R. Uecker, P. Reiche, J. Cryst. Growth, 147 (1995) 123.

[5] R. Jabłoński, I. Pracka, M. Świrkowicz, Proc. of SPIE, 3178 (1997) 303.

[6] R. Jabłoński, S.M. Kaczmarek, I. Pracka, B. Surma, M. Świrkowicz, T. Łukasiewicz, „ESR and optical measurements of $LiNbO_3$ and $LiTaO_3$ single crystals doped with ions of the first transition series", Spectr. Acta Part A 54, (1998 a),1701-1709.

[7] S.M. Kaczmarek, R. Jabłoński, I. Pracka, G. Boulon, T. Łukasiewicz, Z. Moroz, S. Warchoł, „Radiation defects in $SrLaGa_3O_7$ single cystals", Nucl. Instr. and Meth. in Phys. Research B 142, (1998), pp. 515-522.

[8] R. Jabłoński, S.M. Kaczmarek, M. Berkowski, „Radiation defects in $BaLaGa_3O_7$ crystals", Spectr. Acta Part A, (1998 b), 2057-2063.

[9] S.M. Kaczmarek, M. Berkowski, R. Jabłoński, I. Pracka, M. Kwaśny, M. Świrkowicz, Biuletyn WAT, 7-8 (1998 b) 141.

[10] S. M. Kaczmarek, J. Kisielewski, R. Jabłoński, Z. Moroz, M. Kwaśny, T. Łukasiewicz, S. Warchoł., J. Wojtkowska, Biuletyn WAT, 7-8 (1998 c) 113.

[11] P.A. Forrestier, D.F. Sampson, „A new laser line due to energy transfer from color centers to erbium ions in CaF2", Proc. Phys. Soc., 88 (1966), 199-204.

[12] Th. Huber, W. Luthy, H.P. Weber, „Color center to ion energy transfer in $YAlO_3:Er^{3+}$", Optical Communications 147 (1998) 117-120.

[13] S.M. Kaczmarek, A.O. Matkovskii, Z. Mierczyk, K. Kopczyński, D.J. Sugak, A.N. Durygin, Z. Frukacz, Acta Phys. Pol. A, 90 (1996) 285.

[14] S.M. Kaczmarek, M. Kwaśny, M. Malinowski Z. Moroz, Proc. SPIE, 3186 (1997 a) 51.

[15] S.M. Kaczmarek, D.J. Sugak, A.O. Matkovskii, Z. Moroz, M. Kwaśny, A.N. Durygin, "Radiation induced recharging of Ce^{3+} ions in $Y_3Al_5O_{12}$:Nd,Ce single crystals", *Nuclear Instruments and Methods Section B, Beam Interactions with Materials and Atoms* B 132, (1997), pp. 647-652.

[16] Z. Frukacz, T. Łukasiewicz, A.O. Matkovskii, *J. Crystal Growth* 169 (1996) 98-100.

[17] J.T. Randall, M.H.F. Wilkins, Proceedings of the Royal Society of London **A184**, 366 (1945).

[18] W. Drozdowski, K.R. Przegiętka, A.J. Wojtowicz, H.L. Oczkowski, „Charge traps in Ce-doped CaF_2 and BaF_2", Acta Physica Polonica A, vol. 95 (1999).

С.М. КАЧМАРЭК

Radiacionnyje defekty w niekotorych okisnych materialach

Issledowalis spektry absorcii, luminescencii...

S.M. KACZMAREK

Defekty radiacyjne w pewnych materiałach tlenkowych

Streszczenie: W pracy badano widma absorpcji, luminescencji, termoluminescencji i zmiany widm absorpcji i luminescencji, po naświetleniu monokryształów granatów itrowo-aluminiowych, galatów strontowo-gadolinowego oraz barowo-lantanowego i strontowo-lantanowego, niobianu litu oraz tantalanu litu domieszkowanych objętościowo lub dyfuzyjnie ziemiami rzadkimi (Nd, Dy, Er, Tm,

Ho, Pr, Ce, Eu) oraz metalami przejściowymi (Mn, Cr, Cu, Fe), kwantami gamma, elektronami i protonami. Przeprowadzono również pomiary widm EPR przed i po napromieniowaniu badanych kryształów.

Słowa kluczowe: materiałoznawstwo, defekty materiałów, widma, badanie materiałów
Symbole UKD: 548.4